

Nanoscale

Accepted Manuscript



This is an *Accepted Manuscript*, which has been through the Royal Society of Chemistry peer review process and has been accepted for publication.

Accepted Manuscripts are published online shortly after acceptance, before technical editing, formatting and proof reading. Using this free service, authors can make their results available to the community, in citable form, before we publish the edited article. We will replace this *Accepted Manuscript* with the edited and formatted *Advance Article* as soon as it is available.

You can find more information about *Accepted Manuscripts* in the [Information for Authors](#).

Please note that technical editing may introduce minor changes to the text and/or graphics, which may alter content. The journal's standard [Terms & Conditions](#) and the [Ethical guidelines](#) still apply. In no event shall the Royal Society of Chemistry be held responsible for any errors or omissions in this *Accepted Manuscript* or any consequences arising from the use of any information it contains.



Journal Name

ARTICLE

Graphene Homojunction: Closed-edge Bilayer Graphene by Pseudospin Interaction

Received 00th January 20xx,
Accepted 00th January 20xx

Jiaxu Yan,^a Chao Li,^b Da Zhan,^a Lei Liu,^{*c} Dezhen Shen,^c Jer-Lai Kuo,^d Shoushun Chen,^e Zexiang Shen^{*a}

DOI: 10.1039/x0xx00000x

www.rsc.org/

Depending on the sublattices they propagate, the low-energy electrons or holes are labeled with pseudospins. By engineering the pseudospin interaction, we propose that two critical features of a junction, i.e. bandgap opening and spatial charge separation can be realized in graphene layers with proper stacking. We also demonstrate theoretically that such a graphene diode may play a role in the future pseudospin electronics, such as for harvesting the solar energy.

Up to date, many methods have been developed to open bandgap of graphene, including hydrogenation¹, electrically gated bilayer graphene^{2–4}, nanoribbons^{5,6}, defects⁷, graphene-substrate interaction⁸, and absorption of molecules⁹. However, these methods also bring unpleasant side effects to graphene after bandgap opening, such as dramatically increased effective mass, distorted lattice, and damaged layer integrity¹⁰. With such side effects, the resulted graphene will lose its superior transport performance. Another question in making electronic or optoelectronic devices of graphene is how to realize p-n junctions. As graphene is normally p-doped by adsorbates, it is rather hard to be n-doped at the same time¹¹. Although this problem seems being solved by controlling the chemical bonding of graphene nanoribbon edges¹¹, it would be much more desirable to separate the electrons and holes in a more direct and efficient way for device applications. Recently, Liu et al. reported a novel graphene structure that the edge-open AB stacking bilayer graphene transforms to edge-closed AA stacking structure after annealing at extremely high temperature¹². We also experimentally discovered that the zigzag edges of AB stacking bilayer graphene can easily form closed structure even at low temperature annealing condition¹³. In this letter, we further demonstrate theoretically that both obstacles which hinder the electronic application of

graphene can be overcome by properly closing graphene edges.

Fig. 1 (color online). (a) Schematic LE electronic band structure of graphene. (b) Graphene layer with AB stacking folded along zigzag edge. The red (green) ball with a rightward (leftward) pointer represents pseudospin up (down). Only the right part of the supercell is shown for each case. (c) Calculated band structures of AB stacking (top) and AA stacking CEBG (bottom). Insets: Zoom-in of the bandgap regions. k is along Γ -K direction in the unit of $2\pi/a$ (a is lattice constant of graphene).

The equivalence of graphene unit-cell atoms leads its bonding (π) and anti-bonding (π^*) orbitals to touching each other at opposite Brillouin zone corners of K and K', and also gives an extra degree of freedom (i.e. pseudospin) to its low-energy (LE) quasi-particles as shown schematically in Fig. 1a. Being an elementary property, real spins in graphene are inert against the overall morphological changes. However, as a direct product of graphene's lattice symmetry, pseudospins have to comply with the chiral alignment of the graphene sheet and therefore behave differently. For example, after closing its edges, its top and bottom layers may not have the same pseudospin chirality, such as the AB stacking case as shown in Fig. 1b. As the effect of pseudospin interaction is explored in the ascendant by now^{14–17}, the study on the consequent electronic behaviors of graphene would be fundamentally meaningful to the pseudospin physics.

Fig. 2 (color online). DFT eigenvalues (hollow line) and GW quasi-particle energies (solid line) of AA stacking and AB stacking CEBG close to the Dirac point.

In this work, a periodic AB stacking closed edge bilayer graphene (CEBG), as shown in Fig. 1a, is selected to investigate

^a Division of Physics and Applied Physics, School of Physical and Mathematical Sciences, Nanyang Technological University, 637371, Singapore. E-mail: zexiang@ntu.edu.sg

^b College of Physics, Jilin University, Changchun, 130012, People's Republic of China

^c Key Laboratory of Excited State Processes, Changchun Institute of Optics, Fine Mechanics and Physics, Chinese Academy of Sciences, Changchun, 130033, People's Republic of China. E-mail: liulei@ciomp.ac.cn

^d Institute of Atomic and Molecular Sciences, Academia Sinica, Taipei 10617, Taiwan

^e School of Electrical and Electronic Engineering, Nanyang Technological University, Singapore 639798, Singapore

the interlayer pseudospin interaction. In this model, the interlayer distance for the three central carbon hexagons of CEBG is fixed to 3.4 Å which is the typical layer distance of graphite. The first-principles density functional theory calculations were carried out using the Vienna *ab initio* simulation package (VASP)^{18–20}. The electron-ion interaction is described using the projector augmented wave method and the exchange correlation potential using the generalized gradient approximation (GGA) in the Perdew-Burke-Ernzerhof form²¹. The cut-off energy for the basis set was 400 eV. The Brillouin-zone integration was performed within Monkhorst-Pack scheme using a (24×1×1) mesh and the Methfessel-Paxton smearing with a width of 0.2 eV. The model structures containing 120 carbon atoms are optimized with the vacuum separation set to be more than 10 Å, the interlayer distance for the three central carbon hexagons fixed to 3.4 Å, and the total energy converges to 1 meV. Fig. 1c plots the calculated band structure of CEBG, which presents the expected bandgap of 0.113 eV at $k \approx 0.33$. The bandgap for the AB stacking CEBG is crucial, as bilayer graphene is always metallic regardless of its stacking. As the finite curvature of the graphene sheets may also induce energy gaps like in carbon nanotubes²², the role of curved edges in the bandgap opening of AB stacking CEBG has been examined as well. For comparison, we evaluated such edge effect by studying the band structure of the same CEBG model structure, but with AA stacking. As both top and bottom layers in AA stacking CEBG sustain the same chirality, the interlayer pseudospin scattering in AA stacking CEBG will vanish. As shown in Fig. 1a, the conduction band and valence band of AA stacking CEBG intersect at the Dirac point and without presenting bandgap opening. Thus, the contribution from curved edges can be eliminated.

We then use the recently developed van der Waals density functional (vdW-DF)²³ which includes long-range dispersion interactions to investigate the nature of the interlayer bonding in our CEBG models. The optimized geometries using vdW-DF are relatively similar to DFT calculations except some expansions in inter-layer distance for the both cases (AA stacking: 3.759 Å; AB stacking: 3.632 Å). More importantly, as well as the DFT calculations, the vdW-DF calculations give a small gap (0.1eV) for AB stacking and gapless for AA stacking. We compared the energy difference between AB and AA stacking models containing 32 carbon atoms. As expected, the total energy of AB stacking is 0.27 eV/cell lower than that of AA stacking. Next we examine the robustness of our results with respect to a more rigorous approach such as GW approximation²⁴. The G_0W_0 calculations were performed with the YAMBO code²⁵. An affordable super-cell including 32 carbon atoms is adopted. Norm conserving pseudopotentials are expanded in plane-wave basis with a 60 Ry energy cut-off. We choose a 64×1×1 k point sampling. The DFT and GW quasiparticle band structure of our CEBG models close to the Dirac point are shown in Fig. 2. As expected, for AA stacking there is still no gap though GW self-energy corrections usually enlarge the gap. For AB stacking the quasiparticle band structure has a significantly larger band gap (0.7eV) instead of DFT value of 0.3 eV, which is compared with bulk Ge (0.67 eV). Note that

though the supercell studied here is quite small, the conclusion for bigger case is still held. When we consider the Coulomb truncation. For AA stacking there is still no gap, while for AB stacking the quasiparticle band gap (0.5 eV) with the Coulomb truncation is compared to that of without the Coulomb truncation (0.7 eV). Therefore, our previous finding, independently of the level of sophistication, is arguably convincing and sheds new light on graphene research.

Fig. 3 (color online). Calculated band structures of (a) AB stacking and (b) AA stacking CEBG near the Fermi level using DFT data (red dotted lines) and TB models (black dotted lines).

We construct an effective tight binding (TB) model to describe the low energy physics based on the bases $\{p_z, s\}$, where we adopt one p_z projection on each carbon atom, and one s -like projection in the middle of each bond.

$$H_{TB} = \sum_{i,\alpha} \varepsilon_i^\alpha c_i^{\alpha+} c_i^\alpha + \sum_{\langle i,j \rangle, \alpha, \beta} t_{ij}^{\alpha\beta} (c_i^{\alpha+} c_j^\beta + h.c.)$$

Here, ε_i^α represents the on-site energy and $c_i^{\alpha+}$ (c_i^α) is the creation (annihilation) operator of electrons at site i . By fitting with the DFT data, we obtain a series of $t_{ij}^{\alpha\beta}$ hopping parameters. As shown in Fig. 3, the TB model reproduces well the low energy bands. Clearly, the energy spectrum is gapless in AA stacking CEBG but has a finite gap in AB stacking CEBG. Therefore, for the bandgap opening of AB stacking CEBG, the bandgap opening effect arises from the pseudospin interaction only for closing edges. It is worth noting that bandgap opening for AB stacking CEBG originates from a new mechanism which is not suit for pristine open-edge bilayer graphene or graphite. As for open-edge bilayer graphene or graphite, the phases of pseudospins in different layers are not phase correlated and do not carry the exclusive chirality. This point can be seen from Berry phase which is closely attached to pseudospin. The Berry phase for a standing wave near zigzag is trivial whether single layer or bilayer zigzag ribbons^{27–29}. After closing the edges, a nontrivial Berry phase of π appears for CEBG structures, different from the 2π phase of bilayer graphene^{30,31}. This variation from bilayer graphene to CEBG will significantly influence the Hall conductance and deserve a direct evidence for the quantum Hall effect experiments.

Fig. 4 (color online). Density of of CBM electrons and VBM holes of AA stacking CEBG and density of CBM electrons and VBM holes of AB stacking CEBG from top to bottom. The isosurface level set to 0.0003. Red, yellow, purple, and blue colors indicate electron density from higher to lower.

Our theory is valid for these three systems: bilayer graphene (with two open boundaries), folded graphene³² (with one closed boundary), CEBGs or collapsed nanotubes³³ (no open boundaries). For bilayer graphene, the phases of pseudospin in different layers are not phase correlated and do not carry the exclusive chirality. After a single layer graphene is folded or

edges are closed, one can travel from the top layer to the bottom layer and thus leads to interlayer interaction from opposite pseudospin chirality. The mechanism for metal-to-semiconductor transition in collapsed metallic armchair tubes is the physical distinction of the two sublattices^{34,35}, which is invalid for other two systems³⁶. Actually, this mechanism is just a special case of our theory. More generally, based on our theory, any bilayers with different pseudospin chirality will present a gap¹⁸. Indeed, gaps appear in bi-layer graphene even in the absence of external magnetic and electric fields due to electron-electron interactions^{37–44}. Compared with the gap caused by pseudospin interaction, this spontaneous gap that estimated to be of order 1 meV is trivial. Therefore, the features of our finding still remain the same.

We also plot the density distribution of holes at the valence band maximum (VBM) and electrons at the conduction band minimum (CBM) of CEBGs in Fig. 4. The LE states of AA stacking CEBG distribute symmetrically with higher density around the center due to the interlayer coupling. However, for AB stacking CEBG, the symmetric distributions of charge densities break, giving the VBM states on the top left wing and bottom right wing (\backslash style) and the CBM states on the top right wing and bottom left wing ($/$ style). Obviously, such asymmetric charge profiles are energetically favored over the symmetric cases due to the geometrical asymmetry in AB stacking CEBG. This spatial separation of electrons and holes effectively forms a type-II junction without impurity doping and provide the possibility of new charge separation mechanisms, as proposed by Wu *et al.* in tapered or strained silicon nanowires^{45,46}.

Over many years of development of semiconductor electronics, realizing charge separation has always been the critical requirement for application in electronic or optoelectronic devices by *p-n* homojunctions or type II heterojunctions. Here, AB stacking CEBG, which also can be referred to 'type-II homojunction', will remove the technical hurdles of doping in the *p-n* homojunctions and also eliminate deficiencies caused by lattice mismatch at the interfaces in type II heterojunctions. In addition, compared to the tapered or strained silicon nanowires, our CEBG models has more remarkable charms owing to its high carrier mobility and high transparency in graphene. While having the geometrically separated charges and the opened bandgap, the AB stacking CEBG can be used as bricks for developing the future graphene-functionalized electronic devices, such as solar cell.

Here, as shown in Fig. 5a, we propose a multi-folded graphene model derived from AB stacking CEBG. As expected, its energy spectrum has a finite bandgap induced by pseudospin repulsion (see Fig. 5b). Moreover, the density distribution of VBM holes and CBM electrons in Fig. 5c and 5d show similar asymmetric charge separation to that of AB stacking CEBG, where the VBM holes are distributed in ' \backslash ' style and the CBM electrons are distributed in ' $/$ ' style. Fig. 5e illustrates an extremely simple way of harvesting solar energy with the AB stacking CEBG. In this graphene pseudospinronic model device, if illuminated by sunlight, the electrons and holes will be activated separately to the folded edges, alternatively layer by layer due to the chirally AB stacking. To facilitate the

preparation of multi-layer folded graphene models, one can fold graphene flake by introducing anisotropic surface curvature during the synthesis or transfer processes⁴⁷. For example, graphene is firstly transfer onto a metal patterned substrate. Then etching the metal patterns, graphene flakes collapse to form the multi-folded features.

Fig. 5 (color online). (a) Model of multi-folded graphene which is periodic along z- and x-axis. (b) Calculated band structures of multi-folded graphene. Density of CBM electrons (c) and VBM holes (d) of multi-folded graphene. (e) Schematic model device that harvesting solar energy with multi-folded graphene. The isosurface level is set to 0.0003.

In summary, we have shown that AB stacking CEBG exhibit appealing features such as the bandgap opening and spatial charge separation. The former originates from the pseudospin interaction, while the latter arises from geometrical asymmetry.

Concerning the daunting obstacles to opening the bandgap in graphene, the present findings could boost electronic properties of graphene-based devices and pave a novel way towards future pseudospin electronics for harvesting the distinct transport properties of graphene.

Acknowledgements

This research was supported by MOE under AcRF Tier 2 (MOE2012-T2-2-124) and AcRF Tier 3 (MOE2011-T3-1-005) in Singapore.

References

- 1 D. Elias, R. Nair, T. Mohiuddin, S. Morozov, P. Blake, M. Halsall, A. Ferrari, D. Boukhvalov, M. Katsnelson, A. Geim *et al.*, *Science*, 2009, **323**, 610–613.
- 2 T. Ohta, A. Bostwick, T. Seyller, K. Horn and E. Rotenberg, *Science*, 2006, **313**, 951–954.
- 3 J. B. Oostinga, H. B. Heersche, X. Liu, A. F. Morpurgo and L. M. Vandersypen, *Nature materials*, 2008, **7**, 151–157.
- 4 Y. Zhang, T.-T. Tang, C. Girit, Z. Hao, M. C. Martin, A. Zettl, M. F. Crommie, Y. R. Shen and F. Wang, *Nature*, 2009, **459**, 820–823.
- 5 Y.-W. Son, M. L. Cohen and S. G. Louie, *Physical Review Letters*, 2006, **97**, 216803.
- 6 L. Yang, C.-H. Park, Y.-W. Son, M. L. Cohen and S. G. Louie, *Physical Review Letters*, 2007, **99**, 186801.
- 7 X. Peng and R. Ahuja, *Nano Letters*, 2008, **8**, 4464–4468.
- 8 S. Zhou, G.-H. Gweon, A. Fedorov, P. First, W. De Heer, D.-H. Lee, F. Guinea, A. C. Neto and A. Lanzara, *Nature materials*, 2007, **6**, 770–775.
- 9 J. Berashevich and T. Chakraborty, *Physical Review B*, 2009, **80**, 033404.
- 10 L. Liu and Z. Shen, *Applied Physics Letters*, 2009, **95**, 252104.
- 11 X. Wang, X. Li, L. Zhang, Y. Yoon, P. K. Weber, H. Wang, J. Guo and H. Dai, *Science*, 2009, **324**, 768–771.
- 12 Z. Liu, K. Suenaga, P. J. Harris and S. Iijima, *Physical Review Letters*, 2009, **102**, 015501.
- 13 D. Zhan, L. Liu, Y. N. Xu, Z. H. Ni, J. X. Yan, C. Zhao and Z. X. Shen, *Scientific Reports*, 2011, **1**, 12.

- 14 S. H. Abedinpour, M. Polini, A. MacDonald, B. Tanatar, M. Tosi and G. Vignale, *Physical Review Letters*, 2007, **99**, 206802.
- 15 H. Min, G. Borghi, M. Polini and A. H. MacDonald, *Physical Review B*, 2008, **77**, 041407.
- 16 P. San-Jose, E. Prada, E. McCann and H. Schomerus, *Physical Review Letters*, 2009, **102**, 247204.
- 17 M. Trushin and J. Schliemann, *Physical Review Letters*, 2011, **107**, 156801.
- 18 G. Kresse, and J. Hafner, *Physical Review B*, 1993, **47**, 558.
- 19 G. Kresse, and J. Hafner, *Physical Review B*, 1993, **48**, 13115.
- 20 G. Kresse, J. Furthmuller, *Computat. Mater. Sci.*, 1996, **6**, 15.
- 21 J. P. Perdew, K. Burke, and M. Ernzerhof, *Physical Review Letters*, 1996, **77**, 3865.
- 22 M. Ouyang, J.-L. Huang, C. L. Cheung and C. M. Lieber, *Science*, 2001, **292**, 702–705.
- 23 J. Klimeš, D. R. Bowler and A. Michaelides, *Physical Review B*, 2011, **83**, 195131.
- 24 M. S. Hybertsen and S. G. Louie, *Physical Review B*, 1986, **34**, 5390.
- 25 A. Marini, C. Hogan, M. Grüning and D. Varsano, *Computer Physics Communications*, 2009, **180** (8), 1392-1403.
- 26 J. Feng, L. Qi, J. Y. Huang and J. Li, *Physical Review B*, 2009, **80**, 165407.
- 27 C.-H. Park and N. Marzari, *Physical Review B*, 2011, **84**, 205440.
- 28 K.-i. Sasaki, M. Yamamoto, S. Murakami, R. Saito, M. S. Dresselhaus, K. Takai, T. Mori, T. Enoki and K. Wakabayashi, *Physical Review B*, 2009, **80**, 155450.
- 29 K.-i. Sasaki, K. Wakabayashi and T. Enoki, *New Journal of Physics*, 2010, **12**, 083023.
- 30 E. McCann and V. I. Fal'ko, *Physical Review Letters*, 2006, **96**, 086805.
- 31 K. Novoselov, E. McCann, S. Morozov, V. I. Fal'ko, M. Katsnelson, U. Zeitler, D. Jiang, F. Schedin and A. Geim, *Nature Physics*, 2006, **2**, 177–180.
- 32 D. Rainis, F. Taddei, M. Polini, G. León, F. Guinea and V. I. Fal'ko, *Physical Review B*, 2011, **83**, 165403.
- 33 N. Chopra, L. Benedict, V. Crespi, M. Cohen, S. Louie and A. Zetti, *Nature*, 1995, **377**, 135–138.
- 34 P. E. Lammert, P. Zhang and V. H. Crespi, *Physical Review Letters*, 2000, **84**, 2453–2456.
- 35 J.-Q. Lu, J. Wu, W. Duan, F. Liu, B.-F. Zhu and B.-L. Gu, *Physical Review Letters*, 2003, **90**, 156601.
- 36 J.-Q. Lu, J. Wu, W. Duan, B.-L. Gu and H. Johnson, *Journal of Applied Physics*, 2005, **97**, 114314.
- 37 H. Min, G. Borghi, M. Polini and A. H. MacDonald, *Physical Review B*, 2008, **77**, 041407.
- 38 R. Nandkishore and L. Levitov, *Physical Review Letters*, 2010, **104**, 156803.
- 39 F. Zhang, J. Jung, G. A. Fiete, Q. Niu and A. H. MacDonald, *Physical Review Letters*, 2011, **106**, 156801.
- 40 Y. Lemonik, I. Aleiner, C. Toke and V. Fal'ko, *Physical Review B*, 2010, **82**, 201408.
- 41 J. Martin, B. E. Feldman, R. T. Weitz, M. T. Allen and A. Yacoby, *Physical Review Letters*, 2010, **105**, 256806.
- 42 W. Bao, Z. Zhao, H. Zhang, G. Liu, P. Kratz, L. Jing, J. Velasco Jr, D. Smirnov and C. N. Lau, *Physical Review Letters*, 2010, **105**, 246601.
- 43 R. T. Weitz, M. Allen, B. Feldman, J. Martin and A. Yacoby, *Science*, 2010, **330**, 812–816.
- 44 A. Mayorov, D. Elias, M. Mucha-Kruczynski, R. Gorbachev, T. Tudorovskiy, A. Zhukov, S. Morozov, M. Katsnelson, A. Geim and K. Novoselov, *Science*, 2011, **333**, 860–863.
- 45 Z. Wu, J. Neaton and J. C. Grossman, *Physical Review Letters*, 2008, **100**, 246804.
- 46 Z. Wu, J. Neaton and J. C. Grossman, *Nano Letters*, 2009, **9**, 2418–2422.
- 47 K. Kim, Z. Lee, B. D. Malone, K. T. Chan, B. Alemán, W. Regan, W. Gannett, M. F. Crommie, M. L. Cohen and A. Zettl, *Phys. Rev. B*, 2011, **83**, 245433.

Fig. 1

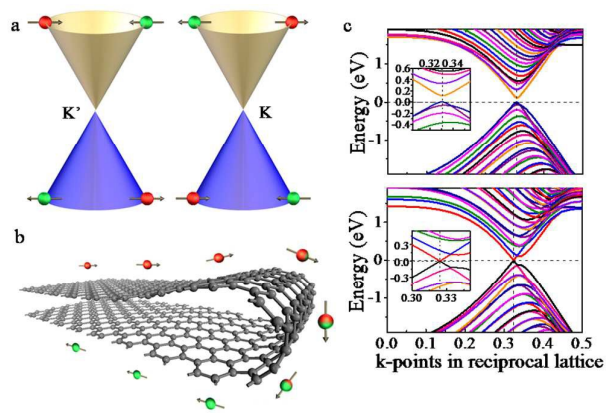


Fig. 2

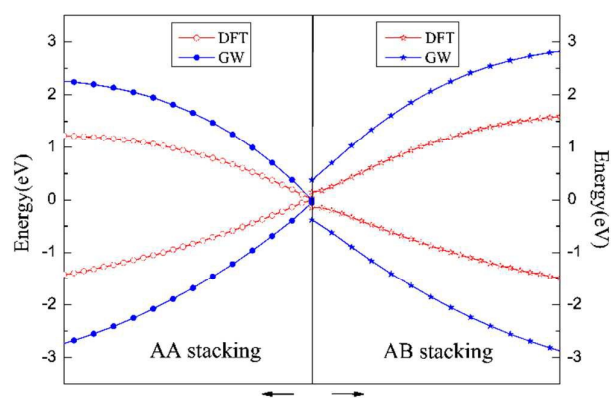


Fig. 3

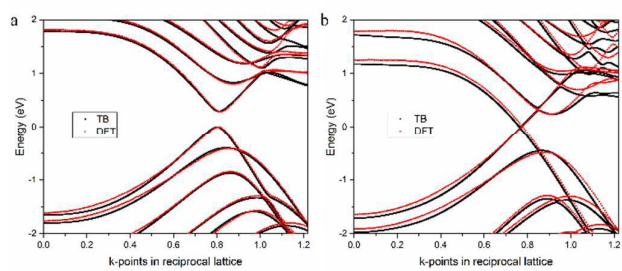


Fig. 4

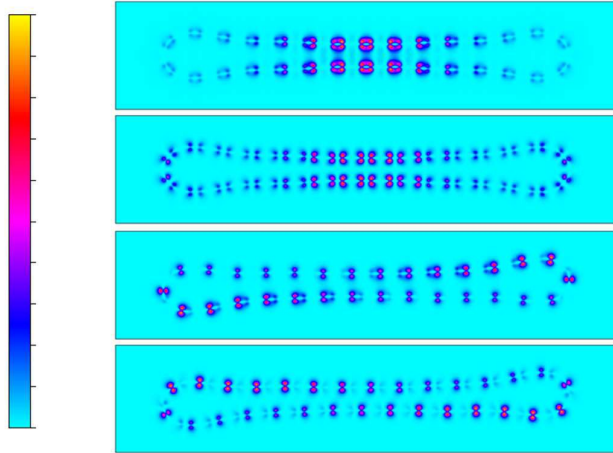


Fig. 5

